 [DOI: 10.1121/1.2963048] Published Online 28 August 2008

Observations of the R reflector and sediment interface reflection at the Shallow Water '06 Central Site

Jee Woong Choi
Department of Environmental Marine Sciences, Hanyang University, 1271 Sa-3-dong, Ansan, Korea
choijw@hanyang.ac.kr

Peter H. Dahl
Applied Physics Laboratory, University of Washington, 1013 NE 40th Street, Seattle, Washington 98105-6698
dahl@apl.washington.edu

John A. Goff
Institute for Geophysics, Jackson School of Geosciences, University of Texas at Austin, JJ Pickle Research Campus, Bldg. 196 (ROC), 10100 Burnet Rd. (R2200), Austin, Texas 78758-4445
goff@ig.utexas.edu

Abstract: Acoustic bottom-interacting measurements from the Shallow Water '06 experiment experiment (frequency range 1–20 kHz) are presented. These are co-located with coring and stratigraphic studies showing a thin (~20 cm) higher sound speed layer overlaying a thicker (~20 m) lower sound speed layer ending at a high-impedance reflector (R reflector). Reflections from the R reflector and analysis of the bottom reflection coefficient magnitude for the upper two sediment layers confirm both these features. Geoacoustic parameters are estimated, dispersion effects addressed, and forward modeling using the parabolic wave equation undertaken. The reflection coefficient measurements suggest a nonlinear attenuation law for the thin layer of sandy sediments.

PACS numbers: 43.30.Cq, 43.30.Ma, 43.30.Pc [WC]
Date Received: March 13, 2008 **Date Accepted:** May 31, 2008

1. Introduction

This paper presents results of measurements of bottom reflection made at frequencies 1–20 kHz, at location 39.0245 N, 73.0377 W (depth 80 m), near the shelf break on the New Jersey continental shelf. This location was the center point of a nominally 1 km^2 area defined as the central site for (mid-frequency) experimental observations [Fig. 1(a)] as part of the Shallow-Water '06 experiment, hereafter referred to as SW06.

Studies originating from previous experiments conducted on the New Jersey shelf, such as those involving the Shallow Water Acoustics in Random Media (SWARM) experiment site[1] and Atlantic Margin Coring Project (AMCOR) site,[2–4] offer potential comparisons with these results, in addition to providing the necessary background for understanding the marine geology and ocean acoustic properties of this continental shelf region. However, the SW06 results reported here involve a much higher frequency than those used in previous studies, and they are also highly localized to within a 0.3-km radius of the above location that is southwest of the vertical line array position of Woods Hole Oceanographic Institution (WHOI) during the SWARM experiment by 26 km, and southeast of the AMCOR borehole No. 6010 site by 7 km. Seabed heterogeneity on the New Jersey shelf is strong over these scales;[5] in particular, the AMCOR site is on a sand ridge, whereas the SW06 central site is on the clay-rich outer-shelf sediment wedge.[6] At this SW06 site, seafloor sand is confined to a thin (~20 cm) winnowed layer[5,7] rather than to a thicker, O(1) m, sand sheet typical of sand ridge sites.[5,6] For these reasons, the initial comparison of our results is limited to the direct *in situ* measurements of

Report Documentation Page

Form Approved
OMB No. 0704-0188

1. REPORT DATE	2. REPORT TYPE	3. DATES COVERED
28 AUG 2008		**00-11-2003 to 00-09-2008**

4. TITLE AND SUBTITLE	5a. CONTRACT NUMBER
Observations of the R reflector and sediment interface reflection at the Shallow Water ’06 Central Site	**N00014-04-1-0111**
	5b. GRANT NUMBER
	5c. PROGRAM ELEMENT NUMBER
6. AUTHOR(S)	5d. PROJECT NUMBER
Jee Woong Choi; Peter Dahl; J Goff	5e. TASK NUMBER
	5f. WORK UNIT NUMBER
7. PERFORMING ORGANIZATION NAME(S) AND ADDRESS(ES)	8. PERFORMING ORGANIZATION REPORT NUMBER
Applied Physics Laboratory,Henderson Hall 355640,1013 NE 40th St.,Seattle,WA,98105-6698	
9. SPONSORING/MONITORING AGENCY NAME(S) AND ADDRESS(ES)	10. SPONSOR/MONITOR’S ACRONYM(S)
Office of Naval Research, 875 N. Randolph St., Arlington, VA, 22203-1995	**APL-UW**
	11. SPONSOR/MONITOR’S REPORT NUMBER(S)

12. DISTRIBUTION/AVAILABILITY STATEMENT

Approved for public release; distribution unlimited

13. SUPPLEMENTARY NOTES

14. ABSTRACT

Abstract: Acoustic bottom-interacting measurements from the Shallow Water ?06 experiment experiment (frequency range 1?20 kHz) are presented. These are co-located with coring and stratigraphic studies showing a thin (~20 cm) higher sound speed layer overlaying a thicker (~20 m) lower sound speed layer ending at a high-impedance reflector (R reflector). Reflections from the R reflector and analysis of the bottom reflection coefficient magnitude for the upper two sediment layers confirm both these features. Geoacoustic parameters are estimated, dispersion effects addressed, and forward modeling using the parabolic wave equation undertaken. The reflection coefficient measurements suggest a nonlinear attenuation law for the thin layer of sandy sediments. (106 words)

15. SUBJECT TERMS

Shallow Water ?06, reflection coefficient, dispersion

16. SECURITY CLASSIFICATION OF:			17. LIMITATION OF ABSTRACT	18. NUMBER OF PAGES	19a. NAME OF RESPONSIBLE PERSON
a. REPORT	b. ABSTRACT	c. THIS PAGE			
unclassified	**unclassified**	**unclassified**	**Same as Report (SAR)**	**7**	

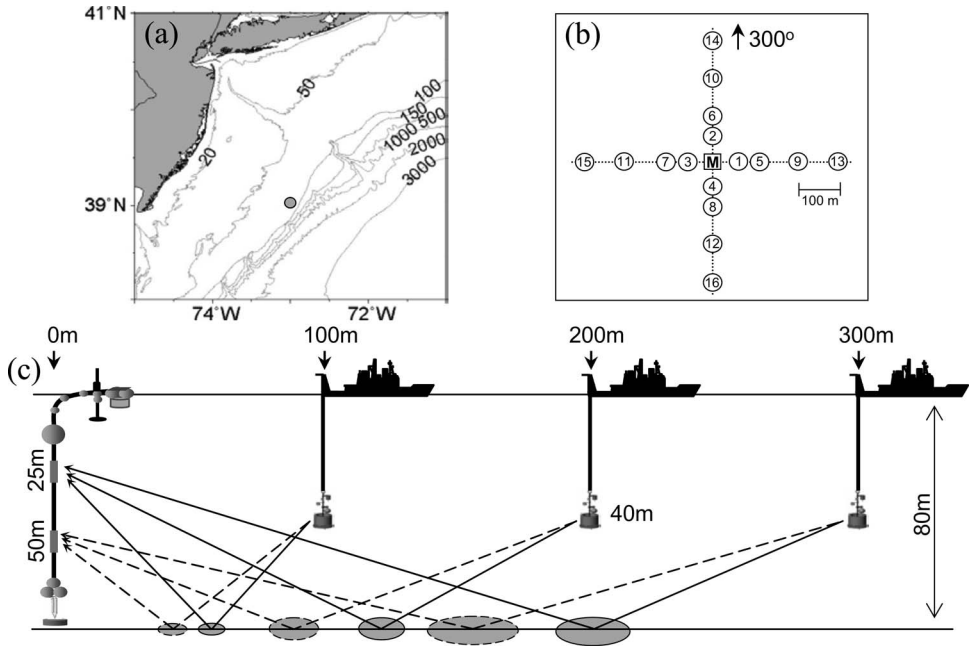

Fig. 1. (a) Experimental location on the New Jersey Shelf (circle) showing isobath contours in meters. (b) Experimental geometry showing 12 source stations along two transects. Source stations 1–4 are used in calibration. The moored receiving array is at the center of set of stations at location M. (c) Geometry showing source position (R/V KNORR) with respect to the receiving array and the resulting set of bottom grazing angles sampled. The ovals represent changing Fresnel zone size, e.g., at 10 kHz the Fresnel zone ranges between 4×4 m at range 100 m to 21×7 m at range 300 m for a receiver depth of 25 m.

sound speed made within the same 0.3 km radius[8] during SW06. Interpretation and forward modeling of our results are guided by the stratigraphic constraints provided by closely spaced (50 m) chirp seismic reflection profiles that provide pseudo three-dimensional coverage of the SW06 central site.[7]

Two kinds of acoustic observations are presented. The first represents a specific, and readily identifiable, single interaction observation of the R reflector, a regionally observed positive-impedance reflector.[7,9,10] Over the SW06 central site the R reflector is at a nominal depth of 22 m based on two-way travel time from the 1–4-kHz vertical incidence chirp data. The R reflector along our SW06 transect lines is relatively flat, changing by at most 3.5 ms ($\sim$3 m) over a span of 1000 m. The multipath corresponding to this reflector is seen in our data in the 1–4-kHz range, and by 6 kHz it has vanished into a background level owing to sediment attenuation. We verify these observations with simulation based on the parabolic equation algorithm.

The second observation is akin to bottom loss, or $-20\log_{10}|R|$, where R is the plane wave reflection coefficient for the seabed. These observations are from a single bottom bounce path that arrives before, and is time resolved from the signal associated with the R reflector. Analysis of arrival times using ray theory shows a perfect match in the timing of this bottom bounce path based on a waterborne path that is reflected once from the bottom. These measurements therefore represent a bottom loss measure restricted to surficial sediments *above* the R reflector. The surficial sediments at this site are fairly coarse ($\sim$1.0–1.3 ϕ medium-coarse sand), with high acoustic velocities (1720–1740 m/s) measured from *in situ* probes at 65 kHz.[5] Coring[7] reveals these coarse seafloor sediments to be confined within a thin ($\sim$20 cm) veneer covering a thicker ($\sim$20 m) layer of very clay rich and lower-velocity sediments ($\sim$1630–1660 m/s, measured at 257 kHz during core logging). The second observation is

therefore identified as a measurement of $-20\log_{10}|R_{13}|$, where R_{13} represents a partial or surficial layer reflection back to the water column (medium 1), from the thin layer (medium 2), and the intervening sediments (medium 3) between it and the R reflector.

2. Experimental description and observations

The acoustic observations were made by a group from the University of Washington Applied Physics Laboratory, from aboard the research vessel R/V KNORR (Knorr Leg-2 of SW06). An acoustic source was deployed at depth 40 m from the stern of the R/V KNORR, and signals were recorded on a moored receiving array system with remotely changeable receiving configuration; in this work signals received on the omni-directional receivers located at depths 25 and 50 m are analyzed. The receiving system was deployed at the above-mentioned coordinates, with this location henceforth referred to as location M.

Measurements were made at stations, defined as the stern position of the R/V KNORR while it underwent precise station keeping using its dynamic positioning system. The stations ranged between 100 and 300 m [Figs. 1(b) and 1(c)] from location M, resulting in a discrete set of six bottom grazing angles between 12.5° and 43.5°. The bearing angle between location M and the R/V KNORR for one transect of stations was 300°, and the other transects are offset this bearing angle by increments of 90°. Measurements were made over the course of the Fig. 1(b) geometry from 10–17 Aug. 2006 at all times of the day. Two types of pulses were used; one a 3-ms continuous wave (cw) pulse for which center frequencies between 4 and 20 kHz were superimposed and transmitted simultaneously on one source (spherical transducer) and the other a 5-ms cw pulse, for which center frequencies between 1 and 4 kHz were superimposed and transmitted simultaneously on another source (flooded-ring transducer, omnidirectional beam in horizontal, 80° beam width in vertical at 3 kHz) activated after a short (~1 s) delay. A particular frequency was recovered in postprocessing via digital bandpass filtering (acoustic data sampled at 50 kHz sampling rate).

For the $-20\log_{10}|R_{13}|$ estimates, the measurements are interpreted as the total acoustic field associated with a *single interaction* with the seabed. This measure represents an average of the squared envelope of received voltage (pressure) taken over 20 pings and averaging in this manner provides an estimate of the squared magnitude of the flat-interface reflection coefficient.[11] An *in situ*, through-the-system, calibration was carried out at four stations located at range 50 m, each separated by 90° in bearing angle (stations 1–4 in Fig. 1). The calibration yielded an estimate of a single, integrated system parameter (ISP) and the variance of ISP (over the course of five days of ISP measurements and over the four bearing angles) forms the major component of measurement uncertainty for estimates of $-20\log_{10}|R_{13}|$. The conductivity-temperature-depth measurements from the R/V KNORR were used to compute ray-based estimates of transmission loss (TL) and seabed grazing angle, θ_g. As a check on the stability of the eigenray paths due to changing sound speed profile, a ray analysis was done for each day from 10–15 Aug. using 15-min-averaged sound speed profiles derived from temperature measurements from a nearby WHOI mooring, generated every 30 s. The analysis showed TL to vary by <0.5 dB and θ_g to vary by $<0.5°$, for the bottom bounce eigenray paths, confirming that our measurements "slip under" and were otherwise not influenced by time-varying water column properties.

Figure 2 summarizes the acoustic observations and displays one of two main results of this paper. A typical sound speed profile [Fig. 2(a)] and the corresponding ray diagram [Fig. 2(b)] show the first six eigenrays delivering the signal over the 200-m range transmission via waterborne paths. These paths in their order of arrival (for 25 m depth receiver) are the direct (D), surface (S), bottom (B), bottom-surface (BS), surface-bottom (SB), and surface-bottom-surface (SBS). The bottom grazing angle, θ_g, for the B path is 25° (19.5° for the 50 m depth receiver). An additional sediment-borne path associated with the R reflector, or R path (R), is depicted in the illustration [Fig. 2(c)].

A time series of the relative received level for a pulse with center frequency 2 kHz [Fig. 2(d)] shows arrival time structure associated with the above paths displayed in Figs. 2(b) and 2(c). The 2-kHz results show a strong R path and additional faint arrivals that we postulate

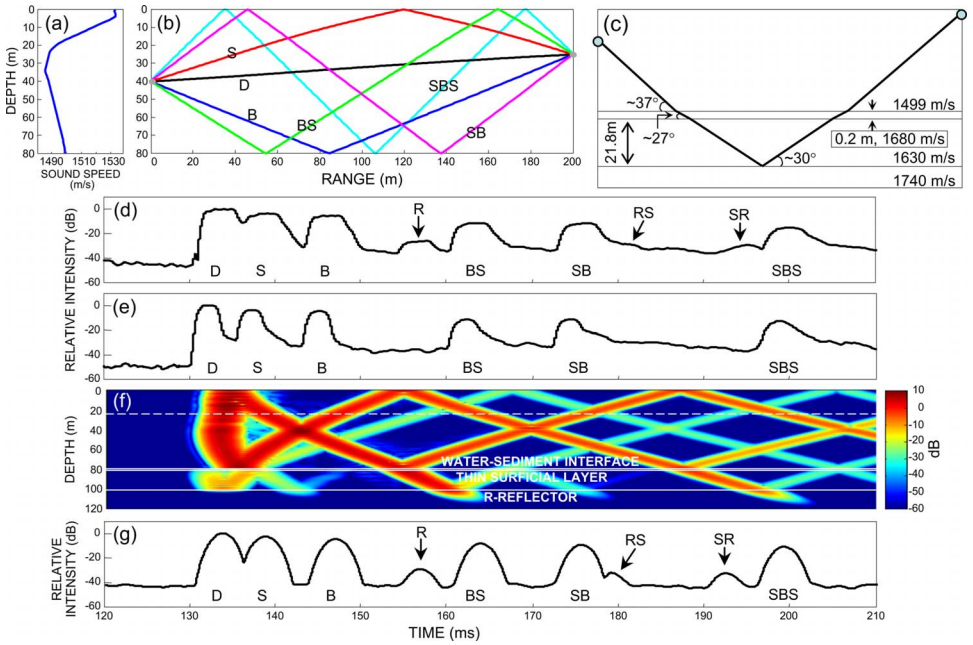

Fig. 2. (a) (Color online) Representative sound speed profile for 10 Aug. 11:07 UTC. (b) Corresponding ray diagram for a source at 40 m, 25 m receiver depth, and range 200 m, showing the first six eigenrays. The third arriving eigenray is the bottom bounce path (B) for which an estimate of $-20\log_{10}|R_{13}|$ is made. Other waterborne paths are the direct (D), surface (S), bottom-surface (BS), surface-bottom (SB), and surface-bottom surface (SBS). (c) An illustration of the sediment-borne path associated with the R reflector (R); the angles noted apply to case of source at 40 m, 25-m receiver depth and range 200 m. (d) Time series of received level for 2-kHz center frequency, based on the average of 20 ping transmissions made on 10 Aug at 10:00 UTC, with acoustic source at station 10 as shown in Fig. 1(b). (e) Simultaneously measured time series of received level for 6 kHz center frequency; here the R path has vanished into the intensity level formed by time spreading of other paths and sediment attenuation. (f) PE-simulated acoustic field (center frequency 2 kHz) for this geometry (see text for description of geoacoustic model used). (g) PE-simulated time series for a source depth at 40 m, receiver depth 25 m, and range 200 m, showing the R-reflector multi-path (R) and additional multi-path species of R-reflector-surface (RS) and surface-R-reflector (SR). Noise has been added to the time series to mimic the nominal, expected ratio for signal-to-background level.

to be R surface (RS) and surface R (SR) paths. In contrast to the 2-kHz results, the R path is not observable in the simultaneously measured 6-kHz results [Fig. 2(e)] as sediment attenuation places this arrival beneath the background level formed by time spreading of prior-arriving paths plus additive noise. The received levels are arbitrarily set to 0 dB for the D path, and an estimate of $-20\log_{10}|R_{13}|$ for the B path is 0.7 dB for 2 kHz and 1.4 dB for 6 kHz.

A calculation performed with a parabolic wave equation (PE) code[12] for this geometry [Fig. 2(f)] shows the acoustic field versus depth and time for a source at depth 40 m, using a 5-ms pulse with center frequency 2 kHz. For the simulation the water column sound speed profile [Fig. 2(a)] is used together with the geoacoustic model in Fig. 2(c). Note: the thin layer sound speed of 1680 m/s corresponds to a dispersion-corrected compressional wave speed at 2 kHz (obtained from Fig. 3 in Ref. 13) of the 1730 m/s speed as determined from *in situ* acoustic measurements at 65 kHz (i.e., mean value of 1720–1740 m/s as mentioned in the introduction). However, in view of the 20-cm-thick layer and 2 kHz frequency, both speeds produce nearly identical results. The most important parameters are the large-layer depth (21.8 m) and speed within this layer (1630 m/s). These are determined from our analysis of the travel time difference between the B and R paths [e.g., as shown in Fig. 2(d)] measured at ranges 200 and 300 m, with an uncertainty in layer depth of ±1 m and speed of ±20 m/s. The densities for the surficial and second layers are assumed to be 2.1 g/cm^3 and 2 g/cm^3 based on core logs made in this area.[14] An empirical relation for compressional wave attenuation within the surfi-

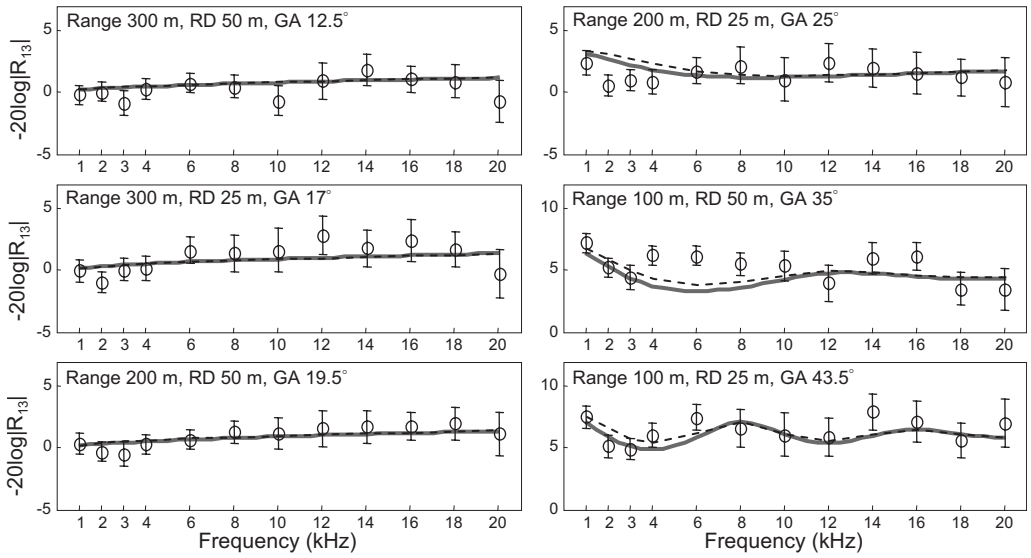

Fig. 3. Measurements of $-20\log_{10}|R_{13}|$ as a function of frequency for six grazing angles (GA) between 12.5° and 43.5°. The grazing angle, source-receiver ranges, and receiver depths (RD) associated with each grazing angle are noted at the top of each plot. The measurements are compared to a two-layered fluid sediment model for which surficial sediment sound speed in the upper (20 cm) layer is 1730 m/s (gray line) and depends on frequency (dashed line) according to a dispersion correction applicable to coarse sand. The frequencies 1, 2, 3, 4, 6, 8, 10, 12, 14, 16, 18, and 20 kHz use 1650, 1680, 1695, 1704, 1711, 1716, 1720, 1723, 1725, 1726, 1727, and 1728 m/s, respectively. Other geoacoustic parameters are discussed in the text.

cial sediment is taken to be $0.2(f/f_{\text{ref}})^{1.6}$ dB/m, where f is a frequency in kHz ($f_{\text{ref}}=1$ kHz), which is a result of the analysis of measurements of $-20\log_{10}|R_{13}|$ as discussed further below and is limited to the frequency range 1–20 kHz. This relation falls within the nominal envelope of attenuation data from sandy sediments corresponding to this frequency range.[11,15]

The attenuation within the second layer is taken to be 0.05 ± 0.01 dB/m/kHz, a value estimated by examining the ratio of amplitudes between the B and R paths for frequencies 1, 2, 3, and 4 kHz, accounting for differences in waterborne TL, assuming reflection and transmission from the three interfaces [shown in Fig. 2(c)] is constant within this narrow frequency band, and taking the total path length within the second layer [Fig. 2(c)] to be 87 m. The attenuation for the thin (20 cm) layer is significantly greater than that used for the larger (~20 m) layer, however a larger attenuation is expected in view of the coarse sand composition of the thin layer.[15]

Finally, the R reflector itself is modeled as a half space with a compressional wave speed of 1740 m/s, density of 2.2 g/cm^3, and attenuation of 0.3 dB/m/kHz, which are taken from inverted values from SW06.[16] The PE calculation clearly shows a reflected field emerging from the layer depth at 22 m—or the R reflector. A cut from this [dashed line in Fig. 2(f)] provides a simulated time series for a receiver depth of 25 m [Fig. 2(g)] that is comparable with data [Fig. 2(d)]. Interestingly, multiple species of the R path, e.g., R-surface (RS), and surface-R (SR) can be seen in both simulation and (faintly) in the 2-kHz data [Fig. 2(d)]. The 2-kHz data and PE simulated time series compare well in terms of timing and arrival structure, supporting a geoacoustic description of the seabed consisting of a thin (~20 cm) surficial layer of higher compressional sound speed, over thicker (~22 m) layer of sediment with slightly lower compressional speed that lies above a higher speed (impedance) reflector, as shown in Fig. 2(c).

The second main result (Fig. 3) are the estimates of the $-20\log_{10}|R_{13}|$ as a function of frequency for the six grazing angles available from the geometry shown in Fig. 1(c) and simul-

taneously measured frequencies between 1 and 20 kHz. The aforementioned two-layer model is compared with these data in two ways. The first (gray line) utilizes 1730 m/s in the thin layer, and second (dashed line) applies a frequency-dependent dispersion correction[13] applicable to coarse sand, for which the sound speed in the thin layer ranges from 1650 m/s at 1 kHz to 1728 m/s at 20 kHz (see figure caption). Both ways utilize the arrival-time inverted estimate of 1630 m/s for the sediments below the thin layer, and the density profiles mentioned in context of Fig. 2. The sediment region below the thin layer is treated as a half space, as the R reflector is time resolved from and not adding to the bottom bounce path, and any impedance change at equivalent subseafloor depths of ~20 m cannot be seen in modeling results at these frequencies. Measurements at the three shallow grazing angles are most sensitive to attenuation within the thin surficial layer, and a nonlinear property of attenuation is suggested by the minor upward slope in $-20\log_{10}|R_{13}|$ estimate with increasing frequency. It is found that the above-mentioned $0.2(f/f_{\mathrm{ref}})^{1.6}$ dB/m relation for the surficial sediment attenuation in this layer provides the best fit to the data.

The dispersion correction yields modest, if any, improvement in view of the variance of the measurements. However, the estimates of $-20\log_{10}|R_{13}|$ are very consistent with the presence of a thin, 20-cm layer overlying a half-space speed of 1630 m/s. Two direct (ground truth) measurements of sound speed were made within a 50 m radius of station 12 [see Fig. 1(b)],[8] using a 2–11-kHz low-frequency (LF) and 10–21-kHz mid-frequency (MF) probe pulse in each case averaging to a depth of 1.6 m into seafloor. In one case the LF and MF speeds were estimated as 1615 and 1622 m/s, respectively, and in the other the LF and MF speeds were estimated as 1598 and 1599 m/s, respectively, with an uncertainty of approximately ±10 m/s applying to all estimates. Given that the 20-cm layer constitutes about 12% of this instrument's averaging depth it is reasonable to assume that these sound speed estimates apply to the region below the 20-cm layer, and are consistent with our corresponding estimate of 1630±20 m/s.

3. Conclusions

The acoustic bottom-interacting measurements from SW06 reported here provide a clear demonstration of the role of stratigraphic constraints and ground truth data on sediment bulk physical properties, on both geoacoustic inversion and acoustic forward modeling. The acoustic measurements made between 1 and 20 kHz are highly localized (within a radius of 300 m) and co-located coring and stratigraphic studies show a thin (~20 cm) higher sound speed layer overlaying a thicker (~20 m) lower sound speed layer ending at a high-impedance reflector (R reflector). The acoustic measurements yielded two key observables: (1) direct measurements of the reflections from the R reflector (for <6 kHz) and (2) estimates of $-20\log_{10}|R_{13}|$ (for 1–20 kHz) from a single bottom bounce path that arrives before, and is time resolved from, the signal associated with the R reflector. In terms of inversion, the R reflector travel time analysis yielded an estimate of the thick layer depth to be 22±1 m within which the compressional wave speed and attenuation were 1630±20 m/s and 0.05±0.01 dB/m/kHz, respectively. Forward modeling using the parabolic equation algorithm reproduced well the arrival structure at 2 kHz.

In contrast, the estimates of $-20\log_{10}|R_{13}|$ are more sensitive to the aforementioned thin, higher speed layer, and the data suggest a nonlinear attenuation law in sandy sediment[17] is more appropriate than a linear one as indicated by the minor upward slope in $-20\log_{10}|R_{13}|$ with increasing frequency at low grazing angles. For the underlying clay-rich sediment layer, a linear frequency-attenuation was estimated by examining the ratio of amplitude between the B and R paths for the 1–4-kHz frequency band, and was utilized in the modeling of $-20\log_{10}|R_{13}|$ for 1–20 kHz within this layer. We do not insist that a linear-frequency dependence apply to the entire 1–20-kHz band, although physical reasons support a linear assumption for such sediments.[17] Finally, and of considerable importance in terms of consistency, the inversion result from the R reflector reflection data, and the modeling result for the $-20\log_{10}|R_{13}|$ estimates, were both reasonably consistent with the co-located direct measurements of sediment sound speed to a depth of 1.6 m.

Acknowledgments

This research was supported by the Office of Naval Research. The mooring No. 54 data used for simulation was made available courtesy of the Woods Hole Oceanographic Institution, Ocean Acoustics Laboratory. UTIG contribution 1989.

References and links

[1]Y.-M. Jiang, N. R. Chapman, and M. Badiey, "Quantifying the uncertainty of geoacoustic parameter estimates for the New Jersey shelf by inverting air gun data," J. Acoust. Soc. Am. **121**, 1879–1894 (2007).
[2]M. V. Trevorrow and T. Yamamoto, "Summary of marine sedimentary shear modulus and acoustic speed profile results using a gravity wave inversion technique," J. Acoust. Soc. Am. **90**, 441–456 (1991).
[3]W. M. Carey, J. Doutt, R. B. Evans, and L. M. Dillman, "Shallow-water sound transmission measurements on the New Jersey continental shelf," IEEE J. Ocean. Eng. **20**, 321–336 (1995).
[4]D. P. Knobles, E. K. Westwood, and J. E. LeMond, "Modal time-series structure in a shallow-water environment," IEEE J. Ocean. Eng. **23**, 188–202 (1998).
[5]J. A. Goff, B. J. Kraft, L. A. Mayer, S. G. Schock, C. K. Sommerfield, H. C. Olson, S. P. S. Gulick, and S. Nordfjord, "Seabed characterization on the New Jersey middle and outer shelf: Correlatability and spatial variability of seafloor sediment properties," Mar. Geol. **209**, 147–172 (2004).
[6]T. A. Davies, J. A. Austin, Jr., M. B. Lagoe, and J. D. Milliman, "Late Quaternary sedimentation off New Jersey: New results using 3-D seismic profiles and cores," Mar. Geol. **108**, 323–343 (1992).
[7]C. Fulthorpe and J. A. Austin, "Shallowly buried, enigmatic seismic stratigraphy on the New Jersey outer shelf: Latest Pleistocene catastrophic erosion?," Geology **32**, 1013–1016 (2004).
[8]J. Yang, D. J. Tang, and K. L. Williams, "Direct measurement of sediment sound speed in Shallow Water '06," J. Acoust. Soc. Am. **124**, EL116–EL121 (2008).
[9]S. P. S. Gulick, J. A. Goff, J. A. Austin, Jr., C. R. Alexander, Jr., S. Nordfjord, and C. S. Fulthorpe, "Basal inflection-controlled shelf-edge wedges off New Jersey track sea-level fall," Geology **33**, 429–432 (2005).
[10]J. D. Milliman, A. Jiezao, L. Anchun, and J. I. Ewing, "Late Quaternary sedimentation on the outer and middle New Jersey continental shelf: Result of two local deglaciations," J. Geol. **98**, 966–976 (1990).
[11]D. R. Jackson and M. D. Richardson, *High-Frequency Seafloor Acoustics* (Springer, New York, 2006).
[12]M. D. Collins, "A split-step Padé solution for the parabolic equation method," J. Acoust. Soc. Am. **93**, 1736–1742 (1993).
[13]K. L. Williams, D. R. Jackson, E. I. Thorsos, D. Tang, and S. G. Schock, "Comparison of sound speed and attenuation measured in a sandy sediment to predictions based on the Biot theory of porous media," IEEE J. Ocean. Eng. **27**, 413–428 (2002).
[14]J. A. Goff, J. A. Austin, Jr., B. Christensen, and A. Turgut, "Chirp seismic reflection data on the New Jersey middle and outer shelf: The geologic response to 40,000 years of sea level change (A)," J. Acoust. Soc. Am. **122**, 2983 (2007).
[15]E. L. Hamilton, "Geoacoustic modeling of the sea floor," J. Acoust. Soc. Am. **68**, 1313–1340 (1980).
[16]Y.-M. Jiang and N. R. Chapman, "Bayesian geoacoustic inversion in a dynamic shallow water environment," J. Acoust. Soc. Am. **123**, EL155 (2008).
[17]J. D. Holmes, W. M. Carey, S. M. Dediu, and W. L. Siegmann, "Nonlinear frequency-dependent attenuation in sandy sediments," J. Acoust. Soc. Am. **121** EL218–EL222 (2007).